

# Secondary caustics in close multiple lenses

V. Bozza

Dipartimento di Scienze Fisiche E.R. Caianiello, Università di Salerno, 84081 Baronissi, Salerno, Italy (valboz@sa.infn.it)  
Istituto Nazionale di Fisica Nucleare, sezione di Napoli

Received 15 February 2000 / Accepted 17 May 2000

**Abstract.** We investigate the caustic structure of a lens composed by a discrete number of point-masses, having mutual distances smaller than the Einstein radius of the total mass of the system. Along with the main critical curve, it is known that the lens map is characterized by secondary critical curves producing small caustics far from the lens system. By exploiting perturbative methods, we derive the number, the position, the shape, the cusps and the area of these caustics for an arbitrary number of close multiple lenses. Very interesting geometries are created in some particular cases. Finally we review the binary lens case where our formulae assume a simple form.

**Key words:** cosmology: gravitational lensing – stars: binaries: close – galaxies: clusters: general – galaxies: quasars: general

## 1. Introduction

The binary Schwarzschild lens is one of the most intensively studied model. In fact, in a relatively simple way, it shows many features that are observed in general gravitational lenses, such as the formation of multiple images, giant arcs and a not trivial critical behaviour. The first study about the binary lens with equal masses was made by Schneider & Weiß (1986). They derived the critical curves and the caustics showing that three possible topologies are present depending on the distance between the two lenses. Erdl & Schneider (1993) extended these results to a generic mass ratio of the two lenses. Witt & Petters (1993) reached the same results using complex notation. In some limits, Dominik (1999) enlightened the connection between the caustics of the binary lens and other models, such as the Chang–Refsdal lens (Chang & Refsdal 1979; 1984) and the quadrupole lens.

The critical curves and the caustics of multiple lenses can develop very complicated structures, so that the attempts to gain some information about them have been very few. However there is a great interest in this problem for its applications in particular situations, such as planetary systems (Gaudi et al. 1998), rich clusters of galaxies and microlensing of quasars by individual stars in the haloes of the lensing galaxies (Chang & Refsdal 1979; Kayser et al. 1988).

In some special situations, the critical curves of multiple lenses can be derived by perturbative methods, referring to the single Schwarzschild lens as the starting point for series expansions (Bozza 1999; Bozza 2000). These methods work very well in planetary systems, for a lens very far from the others and systems where mutual distances are very small with respect to the total Einstein radius. In the first two cases, the complete caustic structure has been derived and the connections with other models have been showed. In the last case, only the central caustic coming up from the deformation of the total Einstein ring has been studied. Besides this main curve, there are many small critical curves forming among the masses. The caustics generated by these curves generally lie far from the centre of mass and can have some influence on sources distant from the mass distribution. Moreover, they move very quickly as the parameters of the system change (Schramm et al. 1993) constituting the most problematic feature to control in numerical simulations. For these reasons they are sometimes dubbed *ghost caustics*. In rapidly rotating binaries they may have superluminal projected motion requiring a non-static treatment of light deflection (Zheng & Gould 2000).

In this paper we use complex notation to face the problem of secondary caustics of close multiple lenses. In this way we can study them as deeply as the other caustics, completing the previous works. We shall see that different classes of secondary caustics can be recognized, showing different geometries.

After some review of multiple lensing in Sect. 2, in Sect. 3 we calculate the number and the position of secondary critical curves for an arbitrary number and configuration of lenses. Then, in Sect. 4, we treat the simple caustics and in Sect. 5 the multiple caustics (the distinction will be explained at the end of Sect. 3). In Sect. 6 we specify our formulae for the binary case and in Sect. 7 we give the summary.

## 2. Basics of multiple lensing

We shall study a system of  $n$  point-lenses placed at positions  $\mathbf{x}_i = (x_{i1}; x_{i2})$  in coordinates normalized to the Einstein radius

$$R_E^0 = \sqrt{\frac{4GM_0}{c^2} \frac{D_{LS}D_{OL}}{D_{OS}}}, \quad (1)$$

where  $M_0$  is a reference mass (it can be chosen to be the total mass, the typical mass of a single object or anything else). The source coordinates  $\mathbf{y} = (y_1; y_2)$  are normalized to the scaled Einstein radius  $R_{E \frac{D_{\text{OS}}}{D_{\text{OL}}}}^0$ . The masses  $m_i$  of the lenses are measured in terms of  $M_0$ .

We introduce the complex coordinate in the lens plane  $z = x_1 + ix_2$  and the complex source coordinate  $y = y_1 + iy_2$ . The positions of the masses will be denoted by  $z_i = x_{i1} + ix_{i2}$ . We also introduce the functions

$$S_k(z) = \sum_{i=1}^n \frac{m_i}{(z - z_i)^k}. \quad (2)$$

The lens equation for our system of  $n$  masses reads (Witt 1990)

$$y = z - \bar{S}_1(\bar{z}). \quad (3)$$

Given a source at position  $y$ , the  $z$ 's solving this equation are the images produced by gravitational lensing.

This map is locally invertible where the determinant of the Jacobian matrix

$$\det J = 1 - \frac{\partial y}{\partial \bar{z}} \frac{\partial \bar{y}}{\partial z} = 1 - |S_2(z)|^2 \quad (4)$$

is different from zero. The points where the Jacobian determinant vanishes are arranged in smooth closed curves called critical curves. The images of these points through the lens map (3) in the source plane are called caustics. When a source crosses a caustic, creation or destruction of pairs of images occurs and the magnification diverges (Schneider et al. 1992).

This is all we need to start our search for secondary caustics in close multiple systems. The fundamental hypothesis we make is

$$|z_i| \ll \sqrt{M} \quad \forall i, \quad (5)$$

where  $M$  is the total mass of the system. In this way, the distances between pairs of lenses will be very small with respect to the Einstein radius of the lens that we would have if all the masses were concentrated at the origin. This Einstein radius is  $\sqrt{M}$  in our notation. The relation (5) allows us to consider the  $z_i$ 's as perturbative parameters in a series expansion. Then we can solve the equation  $\det J = 0$  at each order, writing its solutions as series expansions in powers of the perturbative parameters. In this way we shall find the critical curves of this system and study their properties analytically.

### 3. Number and positions of secondary critical curves

Close multiple lenses have two classes of critical curves: the main critical curve, resulting from the deformation of the Einstein ring of the total mass lens, and the secondary critical curves, forming inside the distribution of the masses.

Effectively, if we multiply the equation  $\det J = 0$  by the quantity  $\prod_{i=1}^n |z - z_i|^4$ , we get a complex equation in  $z$  and  $\bar{z}$ :

$$\prod_{i=1}^n |z - z_i|^4 - \left| \sum_{i=1}^n m_i \prod_{j \neq i} (z - z_j)^2 \right|^2 = 0. \quad (6)$$

At the zero order, putting all  $z_i$ 's to zero, this equation becomes

$$|z|^{4n-4} (|z|^4 - M^2) = 0. \quad (7)$$

This equation has the solution  $|z| = \sqrt{M}$ , that is the Einstein ring of the total mass lens. Taking this solution as the starting point of a perturbative expansion, we get the main caustic. The details of this calculation are in (Bozza 2000). But the presence of the solution  $z = 0$  indicates that also this value can be taken as the starting point for another expansion. This is just the value we shall take to find the secondary critical curves.

Having observed the zero order situation, we can start our perturbative approach, searching for the first order solution. Then we write the solution  $z$  as a series expansion:

$$z = z_0 + o(|z_i|), \quad (8)$$

where  $z_0$  is of the first order in  $|z_i|$ . Stopping at the first order, we put  $z = z_0$  in Eq. (6). We see that the first term becomes of order  $4n$ , while the second is of order  $4n - 4$ . Then the latter dominates the first and Eq. (6) is equivalent to

$$\sum_{i=1}^n m_i \prod_{j \neq i} (z_0 - z_j)^2 = 0. \quad (9)$$

This is a polynomial equation of degree  $2n - 2$ . Then, for a system of  $n$  close lenses, there are, at most,  $2n - 2$  points where the Jacobian determinant vanishes (at the first order in  $z_i$ ), corresponding to  $2n - 2$  secondary critical curves. This is the first main result of our work. It is consistent with the binary lens, since two secondary critical curves are predicted by this formula.

Eq. (9) can be solved analytically for two and three lenses, otherwise we have to resort to simple numerical methods. In Sect. 6, we shall specify these and the following results for the binary lens where a manageable expression for the positions of the critical curves is available. For the triple lens, the analytical solutions are too cumbersome to allow a detailed study.

Now, we have a straightforward way to calculate the positions of the secondary critical curves for an arbitrary configuration of close multiple lenses. Then, we can avoid the traditional blind sampling of the Jacobian determinant on the lens plane and reach, by this new method, the full efficiency.

We take the generical solution  $z_0$  of Eq. (9) as the first order term of our expansion. From now on, we use the notation

$$S_k^0 = S_k(z_0). \quad (10)$$

As both  $z_0$  and  $z_i$  are of the first order, according to our perturbative expansion,  $S_k^0$  has all denominators of order  $k$  and then it is of order  $-k$ .

To continue our study we do not need an analytical expression for  $z_0$ . We shall just use the fact that  $z_0$  is a solution of Eq. (9), that is equivalent to say that

$$S_2^0 = 0. \quad (11)$$

Of course, we have to distinguish between simple roots of Eq. (9) and roots of higher multiplicity. Remembering that the

$k^{\text{th}}$  derivative of  $S_2(z)$  is proportional to  $S_{k+2}(z)$ , we have the equivalence between the following statements:

$$z_0 \text{ is a root of multiplicity } p \Leftrightarrow S_{k+2}^0 = 0 \quad \forall k < p. \quad (12)$$

We shall treat separately the caustics coming from simple roots (hereafter called simple caustics) and the caustics coming from multiple roots (hereafter multiple caustics).

#### 4. Simple caustics

These caustics are largely the most common as we explain in the next section. So they surely have the most practical interest.

##### 4.1. Shape of the critical curves

Once found the positions of the critical curves, we can carry on our perturbative expansion to discover the shape of these curves. So we put

$$z = z_0 + \epsilon_2 + \epsilon_3 + \dots, \quad (13)$$

where  $z_0$  is the position of one simple critical curve, found by Eq. (9), and  $\epsilon_j$  are the corrections of order  $|z_i|^j$ . It is convenient to use the original equation  $\det J = 0$ , which can be written in the form

$$1 - S_2(z_0 + \epsilon_2 + \epsilon_3) \bar{S}_2(\bar{z}_0 + \bar{\epsilon}_2 + \bar{\epsilon}_3) = 0, \quad (14)$$

starting from Eq. (4)

The expansion of  $S_2$  is

$$S_2(z_0 + \epsilon_2 + \epsilon_3) = S_2^0 + \begin{aligned} & -2\epsilon_2 S_3^0 + \\ & -2\epsilon_3 S_3^0 + 3\epsilon_2^2 S_4^0 + \dots \end{aligned} \quad (15)$$

The first row is the order  $-2$  and is null according to Eq. (11). The second row is the order  $-1$  and the third row is the order zero. Inserting this expansion in (14), the lowest order equation is of order  $-2$ :

$$-4|\epsilon_2|^2 |S_3^0|^2 = 0, \quad (16)$$

Being  $z_0$  a simple root,  $S_3^0 \neq 0$ , so that  $\epsilon_2 = 0$ .

The successive terms in the expansion of the equation (14) are of order zero:

$$1 - 4|\epsilon_3|^2 |S_3^0|^2 = 0. \quad (17)$$

From this equation we have

$$|\epsilon_3| = \frac{1}{2|S_3^0|}. \quad (18)$$

Then the third order contains the first information on the shape of the critical curve. Eq. (18) tells us that the critical curve at position  $z_0$  is a circle centered on  $z_0$  with radius

$$r = \frac{1}{2|S_3^0|}. \quad (19)$$

From the form of  $S_3^0$  (see Eq. (2)), we see that the closer the critical curve is to some mass, the higher the value of  $S_3^0$ , the smaller the radius of the circle.

If we multiply all masses by a factor  $\lambda$ , the positions of the critical curves do not change, because  $\lambda$  factors out from Eq. (9), but their radii change as  $\lambda^{-1}$ . If we do the same with the positions of the masses instead, the positions of the critical curves scale as  $\lambda$  and their radii scale as  $\lambda^3$ .

##### 4.2. Caustics

To find the caustics corresponding to the simple critical curves, we just have to put the critical curve, in its obvious parameterization

$$z(\theta) = z_0 + r e^{i\theta} \quad 0 \leq \theta < 2\pi, \quad (20)$$

into the lens equation (3) and expand to the third order:

$$y(\theta) = -\bar{S}_1^0 + z_0 + \left( r e^{i\theta} - \frac{e^{-2i\theta}}{S_3^0} \right). \quad (21)$$

We can observe that the lowest order is  $-1$  and is independent of  $\theta$ . It represents the position of the caustic. From the order of this term, we can deduce that these caustics can lie very far from the origin of our system, going to infinity as the distances among the masses are reduced to zero. The successive term is  $z_0$ , which is of the first order and represents a correction to the position. Finally, the shape of the caustic is given by the third order.

The cusps of a caustic are characterized by the vanishing of the tangent vector. To find them, we have to require that

$$\frac{dy(\theta)}{d\theta} = 0 \quad (22)$$

and solve for  $\theta$ . Taking  $y(\theta)$  from Eq. (21), this equation can be simplified into

$$e^{3i\theta} + \sqrt{\frac{S_3^0}{S_3^0}} = 0, \quad (23)$$

whose solutions are

$$\theta_k = -\frac{1}{3} \arg(S_3^0) + \frac{2k\pi}{3} \quad k = 0, 1, 2, \quad (24)$$

where  $\arg$  yields the argument of a complex number.

We have three cusps. So, in any close multiple system, having only simple secondary caustics, these caustics have a triangular shape.

Finally, we calculate the area of these caustics. This can be done by the integral

$$A = \int_{\gamma} y_2 dy_1, \quad (25)$$

where  $\gamma$  is the caustic in its clockwise direction. We have

$$A = -\frac{1}{4i} \int_0^{2\pi} [y(\theta) - \bar{y}(\theta)] \partial_{\theta} [y(\theta) + \bar{y}(\theta)] d\theta. \quad (26)$$

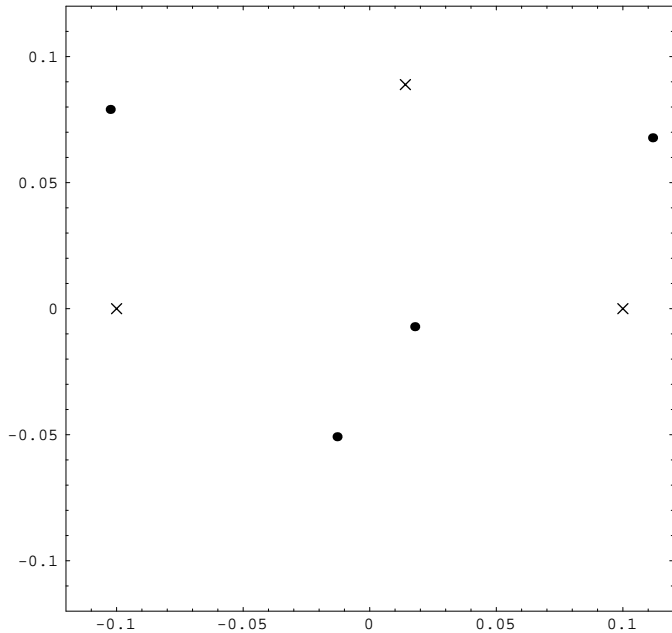


**Fig. 1.** Positions of the four secondary critical curves (indicated by the small dots) for a triple system with masses  $m_1 = 0.25$ ,  $m_2 = 0.25$ ,  $m_3 = 0.5$  and positions  $z_1 = 0.1$ ,  $z_2 = -0.1$ ,  $z_3 = 0.014 + i0.089$  (indicated by the three crosses).

The minus in the right member comes from the fact that our parameterization is counterclockwise. The integral only involves complex exponential functions and the result is

$$A = \frac{1}{2} \pi r^2. \quad (27)$$

So the extension of the simple caustics is of the sixth order in the separations among the lenses, justifying the evasive nature of these caustics.

With our expansions, we have attained considerable analytical information about the secondary caustics establishing their shape, the area, the number of cusps in a completely general way. However, since these results are the fruit of perturbative approximations, it is important to discuss their accuracy. So we propose a comparison between our perturbative results and the numerical ones in a typical situation. We consider a system constituted by three lenses disposed as in Fig. 1. According to our previous statement, this system can form, at most, four simple secondary critical curves. For our choice of parameters, we display their positions in the same figure. The caustics produced by these curves are shown in Fig. 2 where they are compared to the numerical ones. We have taken the distances among the masses of this distribution to be one tenth of the total Einstein radius. Even for this not too small value, the positions and the shapes of the secondary caustics are reproduced with a striking accuracy. It is also to be noted that the quality of numerical results is improved thanks to the guide provided by perturbative results.

So we see that the analytical formulae derived in this section are very good approximations to the quantitative characteristics of the secondary caustics, proving to be highly reliable.

## 5. Multiple caustics

In this section, we consider the case where  $z_0$  is a multiple root of Eq. (9). The parameters space of a system with  $n$  lenses is  $3n - 4$  dimensional, since each mass adds three parameters (its mass and its coordinates in the lens plane). Four parameters can be eliminated by considering equivalent those systems differing by a global translation or rotation and/or by a global scale factor. Thus, for example, the binary lens is completely characterized by the mass ratio and the separation between the lenses.

The requirement of a double root in Eq. (9) translates into the vanishing of the derivative of this equation with respect to  $z$ . This is one constraint equation, then the points of the parameters space producing multiple roots constitute a  $3n - 5$  dimensional hypersurface, thus having measure zero. For this reason, the occurrence of multiple roots is relatively rare. Anyway, very interesting features emerge, justifying a detailed study of these particular cases.

### 5.1. Critical curves

Suppose that  $z_0$  is a root with multiplicity  $p$ . We have to find the correct order of the perturbation to insert in the equation  $\det J = 0$ , representing the shape of our critical curve. According to the equivalence (12), the  $S_{k+2}^0$  with  $k < p$  are null. Then, we put

$$z = z_0 + \epsilon, \quad (28)$$

with the order (that we shall indicate by  $q$ ) of  $\epsilon$  to be found. We only assume that  $q$  be higher than one. Then, the expansion of  $S_2(z)$  is

$$S_2(z_0 + \epsilon) = S_2^0 - 2\epsilon S_3^0 + 3\epsilon S_4^0 + \dots \\ \dots + (-1)^k (k+1) \epsilon^k S_{k+2}^0 + \dots \quad (29)$$

The  $k^{\text{th}}$  term is of order  $qk - (k+2)$  and the first term to be non-null is that for  $k = p$ . When we put this expansion in the equation  $\det J = 0$ , the first non-null term is

$$-(p+1)^2 |\epsilon^p S_{p+2}|^2 \quad (30)$$

having order  $2qp - 2(p+2)$ . If this order is less than zero, we just get from  $\det J = 0$  that  $\epsilon = 0$ , but if the order of this term is zero, then the zero order expansion of  $\det J = 0$  also involves another term (equal to 1):

$$1 - (p+1)^2 |\epsilon^p S_{p+2}|^2 = 0 \quad (31)$$

and the equation gives the non-trivial solution

$$|\epsilon| = \frac{1}{[(p+1) |S_{p+2}|]^{1/p}}. \quad (32)$$

This happens when the order of  $\epsilon$  is  $q = \frac{2+p}{p}$ . This is consistent with the result of the previous section, because, for  $p = 1$ ,  $q = 3$ . For  $p = 2$ , we have that the first non trivial order is the second and, for  $p = 3$ , it is the order  $\frac{5}{3}$ . When  $p$  increases, the order of this perturbation decreases, approaching 1 as a limit. This means that at high multiplicities, the perturbative expansion becomes always less accurate, requiring ever more terms for an adequate

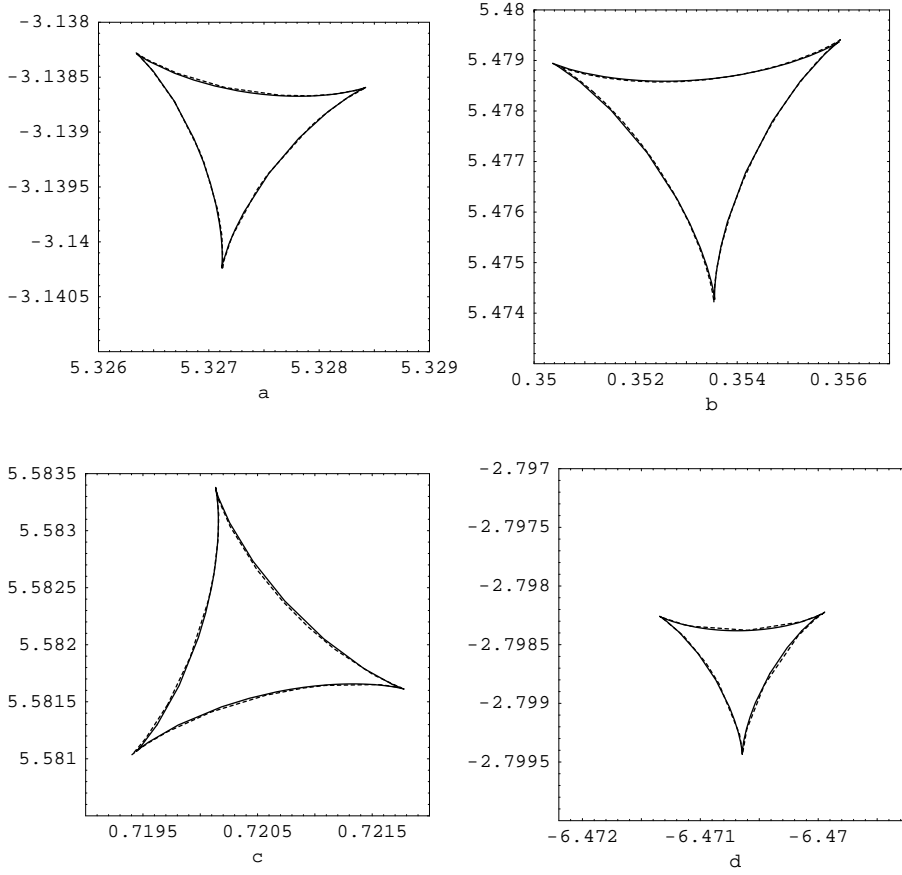


**Fig. 2a–d.** Here are the four caustics produced by the critical curves of Fig. 1 from left to right. The solid curve is the perturbative caustic and the dashed line is the numerical one.

description of the caustics. Anyway, the main characteristics of the caustics can be derived retaining just the first correction and that is what we shall do.

The critical curve just derived is again a circle with radius

$$r = \frac{1}{[(p+1)|S_{p+2}^0|]^{1/p}}, \quad (33)$$

becoming greater with the multiplicity.

## 5.2. Caustics

We take, as before, the parameterization

$$z(\theta) = z_0 + re^{i\theta} \quad (34)$$

for the critical curve, with  $r$  given by Eq. (33). Putting this expression into the lens equation (3) and expanding to the  $q^{\text{th}}$  order, we get

$$y(\theta) = -\bar{S}_1^0 + z_0 + r \left[ e^{i\theta} + (-1)^p \frac{e^{-(p+1)i\theta}}{p+1} \sqrt{\frac{\bar{S}_{p+2}^0}{S_{p+2}^0}} \right]. \quad (35)$$

The  $q^{\text{th}}$  order is the first depending on  $\theta$  and determines the shape of the caustic.

To understand this shape, we calculate the cusps as in the previous section. The equation for the cusps is

$$e^{(p+2)i\theta} + (-1)^{p+1} \sqrt{\frac{\bar{S}_{p+2}^0}{S_{p+2}^0}} = 0 \quad (36)$$

and its solutions are

$$\theta_k = \frac{(-1)^p}{p+2} \arg(S_{p+2}^0) + \frac{2k\pi}{p+2} \quad 0 \leq k < p+2. \quad (37)$$

Now we have  $p+2$  cusps. This is a very interesting result, because the caustic assumes the shape of a regular polygon with  $p+2$  curved sides.

The area of the multiple caustic can be calculated in the same way as for the simple one. We just give the result:

$$A = \frac{p}{p+1} \pi r^2. \quad (38)$$

It is of order  $2 \frac{2+p}{p}$ . So, increasing the multiplicity from 1 to infinity, the order of the area lowers from 6 to 2 and the extension of the caustic becomes ever more important.

Some other consideration about the limit for  $p \rightarrow \infty$  can be done. The number of cusps become infinite and, from Eq. (35), we see that the caustic becomes a circle of radius  $r$ . In fact, the area becomes  $\pi r^2$ .

## 5.3. An example: a double caustic in a triple lens

Now we shall practically see how our formulae work in the case of a multiple caustic. We consider three masses:  $m_1 = 0.25$ ,

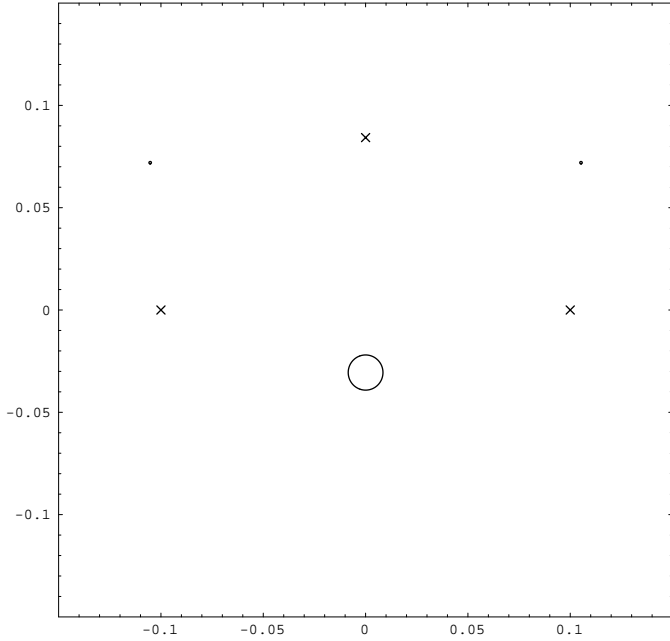


**Fig. 3.** Critical curves in the event of a double root. The masses are indicated by the crosses. The double critical curve is the one at the bottom-center, while the other two are on the top-left and top-right and are hardly visible in this picture.

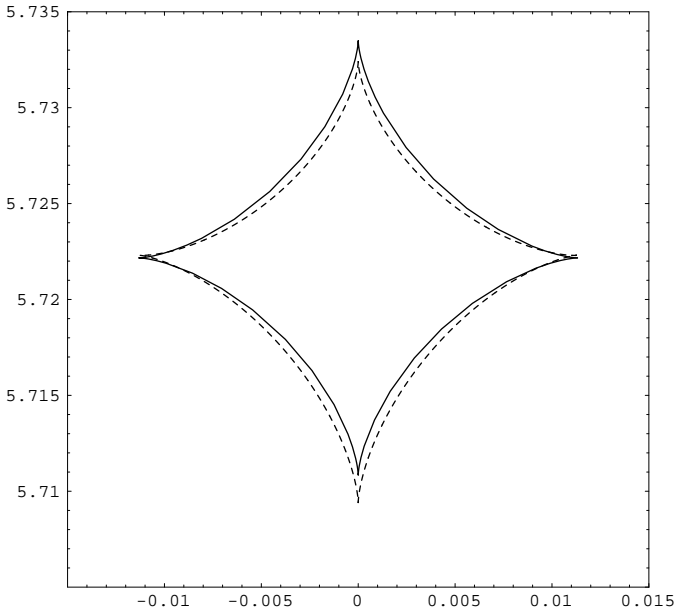


**Fig. 4.** Caustic corresponding to the double critical curve of Fig. 3. The dashed curve is the numerical caustic and the solid line is the perturbative one.

$m_2 = 0.25$  and  $m_3 = 0.5$ . We fix the positions of the first two:  $z_1 = 0.1$ ,  $z_2 = -0.1$ ; but we let the third free for the moment. We simultaneously solve Eq. (9) and its derivative with respect to  $z_0$ , for the two unknowns  $z_0$  and  $z_3$ . We find six possible positions of the third mass, giving rise to a double root of the positions equation. None of them is a triple root. Two of these positions are on the  $x_2$ -axis. We choose one of them:

$z_3 = i0.084263$ . The double root is in  $z_0 = -i0.0299$ . In Fig. 3, we see that the critical curve in this point is much greater than the other two. In fact, the radius of the double critical curve, calculated by Eq. (33), is  $8.49 \times 10^{-3}$ , while the radius of the two simple critical curves is  $6.13 \times 10^{-4}$ , according to Eq. (19).

In Fig. 4, we show the caustic generated by this double critical curve. The geometry is correctly predicted by our perturbative expansion: there are four cusps in a double caustic. We see that the approximation is less accurate than before, as we anticipated in our discussion about the order of the perturbation. However, for double caustics, it is not so difficult to add another term to the perturbative expansion and reach the same accuracy of the simple caustics. The third order term in the critical curve depends on  $\theta$ :

$$\epsilon_3 = 6r^2 \text{Re} \left[ \bar{S}_4^0 S_5^0 e^{i\theta} \right]. \quad (39)$$

The successive term in the caustic is

$$e^{i\theta} \epsilon_3 + 3e^{-3i\theta} r^2 \epsilon_3 \bar{S}_4^0 - r^4 e^{-4i\theta} \bar{S}_5^0. \quad (40)$$

Double caustics, and, more generally, multiple caustics, are formed by the union of small caustics, in some sense. Another interesting question is: what happens if we change the parameters in the neighbourhood of our particular choice producing the double root? We expect the double critical curve to separate into two smaller ovals and the double quadrangular caustic to break into two triangular ones; but this can happen in different ways.

In this regime, the perturbative caustics are simple. However, as the parameters tend to give the double root,  $S_3^0$  tends to zero, yielding a diverging  $r$  for the simple critical curves, according to Eq. (19). The transition with the formation of the double critical curve is thus not reproduced. Guided by perturbative approximations, the break of the double caustic, when  $z_3$  moves out from the position  $i0.084263$ , can be investigated numerically. The results are shown in Fig. 5.

In case *a*,  $z_3 = i0.082787$ , i.e. we have moved the third mass towards the others. The critical curve breaks in the horizontal direction. Looking just at the thick line in Fig. 5a2, representing the numerical caustic, we see that the top cusp and the bottom cusp develop a butterfly geometry. At some critical value, these butterflies touch and the two resulting triangular caustics move away along the horizontal direction. We have displayed in the same plot the perturbative caustics too. Obviously, they are simple caustics, so they cannot show the butterfly geometry but they can help in understanding how the separation occurs. We also notice that the simple caustics cover the area of the numerical transition double caustic very well constituting a significant approximation anyway.

In case *b*,  $z_3 = i0.085759$ , so that the third mass is farther from the others. Now the critical curve breaks in the vertical direction and so does the caustic. The left and the right cusps transform into butterflies. These butterflies are slightly distorted by the fact that the resulting simple caustics have different sizes: the one on the top is smaller than the other.

In case *c*,  $z_3 = 0.00147 + i0.084263$ . We have displaced the third mass in the horizontal direction. The critical curve

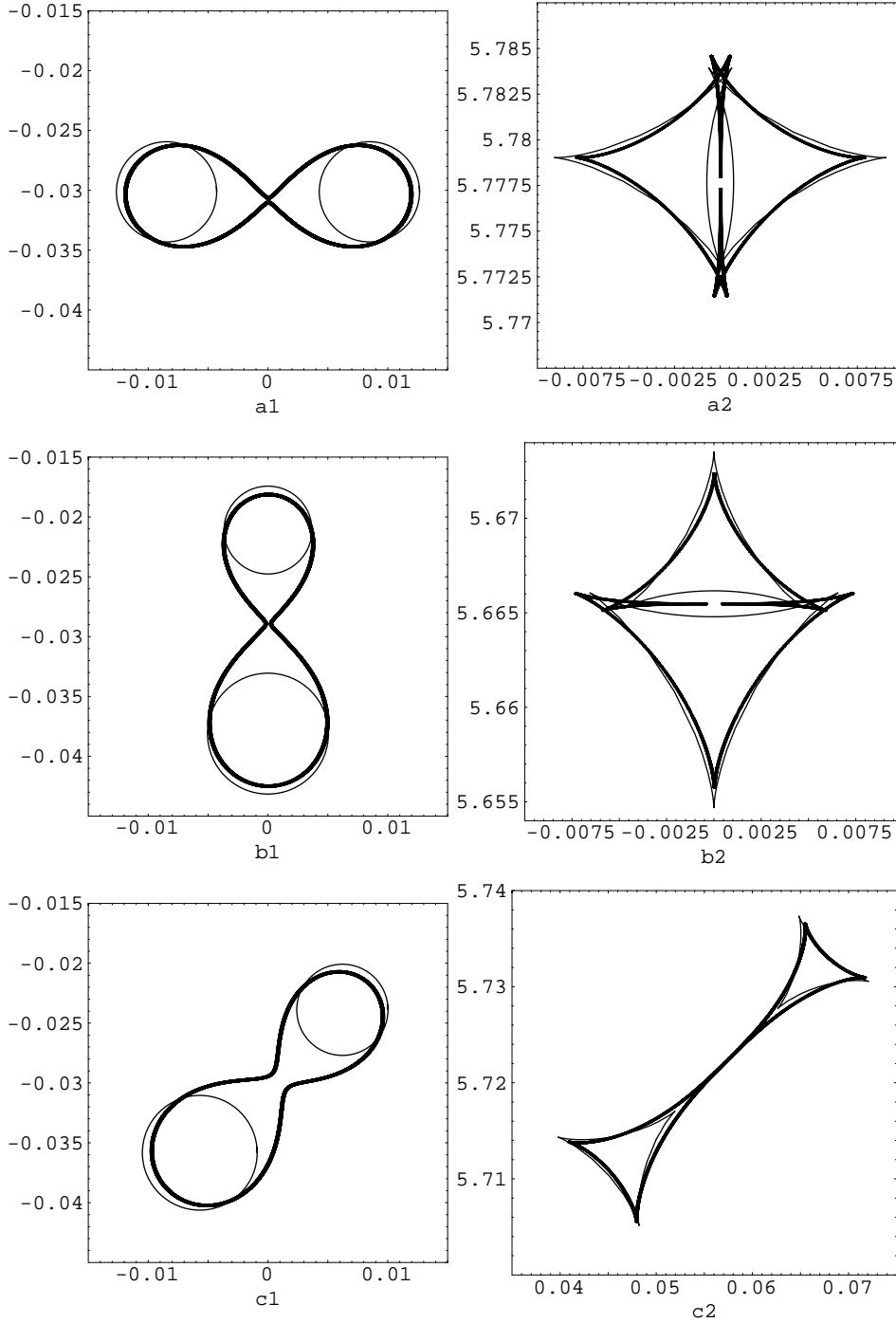


**Fig. 5.** Critical curves and caustics for  $z_3$  close to  $i0.084263$ . The left column shows the critical curves and the right column the caustics. The thick lines are the numerical curves and the thin lines are the perturbative ones. The choice of  $z_3$  in cases *a*, *b* and *c* are given in the text.

breaks diagonally and so does the caustic. But this time the transition occurs with a simple beak-to-beak singularity rather than with butterflies. While in the previous situations the two simple caustics in the last step of the separation touch with a fold, here they touch with a cusp.

## 6. Secondary caustics in binary lensing

In this section, we specify our results for the binary case where simple analytical formulae can be written. Let's consider two masses placed on the horizontal axis and let's choose the origin

in the centre of mass. We call the separation between the masses  $a$ , then we have  $z_1 = \frac{m_2 a}{m_1 + m_2}$  and  $z_2 = -\frac{m_1 a}{m_1 + m_2}$ . Eq. (9) is of second degree. Its solutions are

$$z_0 = a \frac{m_2 - m_1 \pm i\sqrt{m_1 m_2}}{m_1 + m_2}. \quad (41)$$

They are always simple and lie on a circle of radius  $a/2$  centered in the middle of the two masses.

The radius of the two ovals is the same:

$$r = \frac{\sqrt{m_1 m_2} a^3}{2(m_1 + m_2)^2}. \quad (42)$$

Its maximum value  $\frac{a^3}{4M_{\text{tot}}}$  is reached when the two masses are equal, in fact, in this case, their distance from the two masses is maximum.

The two caustics are given by the following expression:

$$y(\theta) = \frac{m_1 - m_2}{a} \mp i \frac{2\sqrt{m_1 m_2}}{a} + a \frac{m_2 - m_1}{m_1 + m_2} \pm ia \frac{\sqrt{m_1 m_2}}{m_1 + m_2} + a^3 \sqrt{m_1 m_2} \times \left[ \frac{e^{i\theta}}{2(m_1 + m_2)^2} \pm \frac{ie^{-2i\theta}}{4(\sqrt{m_1} \pm i\sqrt{m_2})^4} \right]. \quad (43)$$

Their cusps are at positions

$$\theta_k = -\arg \left[ \pm i (\sqrt{m_1} \pm i\sqrt{m_2})^4 \right] + \frac{2k\pi}{3} \quad k = 0, 1, 2. \quad (44)$$

Their area is

$$A = \frac{\pi m_1 m_2 a^6}{8(m_1 + m_2)^4}, \quad (45)$$

reaching the maximum value  $\frac{\pi a^6}{32M_{\text{tot}}^2}$  in the equal masses case.

## 7. Summary

Multiple Schwarzschild lensing represents a very rich terrain for the exploration of caustics in gravitational lensing. The occurrence of different kinds of singularities stimulates new investigations.

In this paper we have applied perturbative methods to secondary caustics, forming when the masses are close each other with respect to the total Einstein radius. In this way we

have been able to establish the number of the caustics for any lens configuration, the positions and the shapes, with a complete characterization of the geometries arising in all cases. Moreover, quantitative formulae for the area and other features of these objects have been given. As we have seen, in the most common case, the shape of the simple caustics is always triangular. Anyway, multiple caustics exist developing a great variety of behaviours, giving rise, to curves having a number of cusps ranging from four to infinity. The breaking of multiple caustics can follow different ways depending on how the parameters of the system change.

*Acknowledgements.* I would like to thank Gaetano Scarpetta and Salvatore Capozziello for their helpful comments on the manuscript. Work supported by fund ex 60% D.P.R. 382/80.

## References

- Bozza V., 1999, A&A 348, 311
- Bozza V., 2000, A&A 355, 423
- Chang K., Refsdal S., 1979, Nat 282, 561
- Chang K., Refsdal S., 1984, A&A 132, 168
- Dominik M., 1999, A&A 349, 108
- Erdl H., Schneider P., 1993, A&A 268, 453
- Gaudi B.S., Naber R.M., Richard M., Sackett P.D., 1998, ApJ 502, 33
- Kayser R., Weiß A., Refsdal S., Schneider P., 1988, A&A 214, 4
- Schneider P., Ehlers J., Falco E.E., 1992, Gravitational lenses. Berlin: Springer-Verlag
- Schneider P., Weiß A., 1986, A&A 164, 237
- Schramm T., Kayser R., Chang K., et al., 1993, A&A 268, 350
- Witt H.J., 1990, A&A 236, 311
- Witt H.J., Petters A.O., 1993, J. Math. Phys. 34, 4093
- Zheng Z., Gould A., 2000, submitted to ApJ, astro-ph/0001199